The Journal of Experimental Biology 216, 1916-1923

doi:10.1242/jeb.083485

RESEARCH ARTICLE

Sex-specific retinal pigmentation results in sexually dimorphic long-wavelength-sensitive photoreceptors in the eastern pale clouded yellow butterfly, *Colias erate*

Yuri Ogawa[1], Michiyo Kinoshita[1], Doekele G. Stavenga[2] and Kentaro Arikawa[1,*]

[1]Laboratory of Neuroethology, Sokendai-Hayama (The Graduate University for Advanced Studies), Hayama 240-0193, Japan and [2]Department of Computational Physics, University of Groningen, Groningen, NL-9747 AG Groningen, The Netherlands

*Author for correspondence (arikawa@soken.ac.jp)

SUMMARY

The compound eyes of the eastern pale clouded yellow butterfly, *Colias erate*, contain three types of ommatidia (I, II and III), identifiable by the differing arrangements of pigment clusters around the rhabdoms. The pigment color is red in all ommatidial types except for type II ommatidia of females, where the pigment is orange. Intracellular recordings demonstrated that the spectral sensitivities of the proximal photoreceptors (R5–8) of all ommatidia in both sexes are strongly tuned by the perirhabdomal pigments. These pigments act as long-pass filters, shifting the peak sensitivities into the wavelength range above 600 nm. Due to the sex-specific pigments in type II ommatidia, the spectral sensitivities of the R5–8 photoreceptors of females peaked at 620 nm while those in males peaked at 660 nm. The measured spectral sensitivities could be well reproduced by an optical model assuming a long-wavelength-absorbing visual pigment with peak absorbance at 565 nm. Whereas the sexual dimorphism was unequivocally demonstrated for the ventral eye region, dimorphism in the dorsal region was not found. Presumably the ventral region is adapted for sexual behaviors such as courtship and oviposition.

Key words: color vision, insect, ommatidium, opsin, spectral sensitivity, visual pigment.

Received 3 December 2012; Accepted 30 January 2013

INTRODUCTION

The eyes of butterflies are composed of thousands of ommatidia, each containing nine photoreceptor cells, R1–9. The visual pigment-containing organelles of these photoreceptors, the rhabdomeres, are closely apposed and thus form a fused rhabdom. In many butterflies, specifically pierids and papilionids, the rhabdom is tiered. The distal tier is made up of the rhabdomeric microvilli of four distal photoreceptors (R1–4), and the proximal tier consists of the microvilli of four proximal photoreceptors (R5–8). At the base of the rhabdom, the basal photoreceptor, R9, contributes a few additional microvilli (Fig. 1).

The spectral sensitivities of the photoreceptors are principally determined by their visual pigments, but may be modified by additional optical effects. Notably, clusters of pigment granules that are concentrated near the light-guiding rhabdoms act as long-pass filters and thus can shift the spectral sensitivity of the photoreceptors. Detailed studies on the small white butterfly, *Pieris rapae* (Pieridae), identified clusters of pale red and deep red pigments located inside the photoreceptors, adjacent to the rhabdoms. These pigments cause a pronounced shift towards red in the spectral sensitivity of the proximal photoreceptors. Whereas all proximal photoreceptors express a visual pigment with an absorption spectrum peaking in the green range at around 560 nm, photoreceptors in ommatidia with pale-red pigment have a spectral sensitivity peaking at 620 nm, and those in ommatidia with deep-red pigment have a peak sensitivity of 640 nm (Qiu and Arikawa, 2003; Wakakuwa et al., 2004). The receptors are accordingly termed red (R) and deep-red (dR) receptors.

When observed with an epi-illumination microscope, the eyes of most butterflies (with the exception of all papilionids and some pierids) exhibit a striking eyeshine, due to the presence of a tracheal tapetum at the bottom of the rhabdom (Fig. 1) (Arikawa and Stavenga, 1997; Bernard and Miller, 1970; Takemura et al., 2007). The tapetum reflects light that has escaped absorption while propagating through the rhabdom. Some of the reflected light travels back through the rhabdom and leaves the eye, and is visible as the eyeshine. The eyeshine spectrum (that is, the reflectance spectrum of the individual ommatidium) depends on the absorption by the visual pigments as well as the spectral filtering by the pigment clusters surrounding the rhabdoms, and thus the eyeshine color is a useful indicator of the type of ommatidium. In *P. rapae*, the individual ommatidia have eyeshine peaking at 635 or 675 nm. By a combination of histological, optical and electrophysiological methods, it could be demonstrated that ommatidia with reflectance spectra peaking at 635 nm contained 620 nm-peaking R-receptors and ommatidia with eyeshine peaking at 675 nm contained 640 nm-peaking dR-receptors (Qiu and Arikawa, 2003).

In the pale clouded yellow butterfly, *Colias erate* (Pieridae), we have recently found that the eyeshine spectrum peaks near the infrared, at 730 nm, in a subset of ommatidia, suggesting that their photoreceptors may have a spectral sensitivity peaking at an even longer wavelength than those of *P. rapae*. We therefore decided to perform an extensive study of the *C. erate* eye, involving anatomical (Arikawa et al., 2009), molecular biological (Awata et al., 2009) and physiological (Pirih et al., 2010) analyses. We previously investigated the distal photoreceptors and found a clear sexual dimorphism due to sex-specific pigmentation of the ommatidia (Ogawa et al., 2012). Here we report a subsequent study on the properties of the proximal photoreceptors, with particular reference to the sexual dimorphism in their spectral sensitivities. We

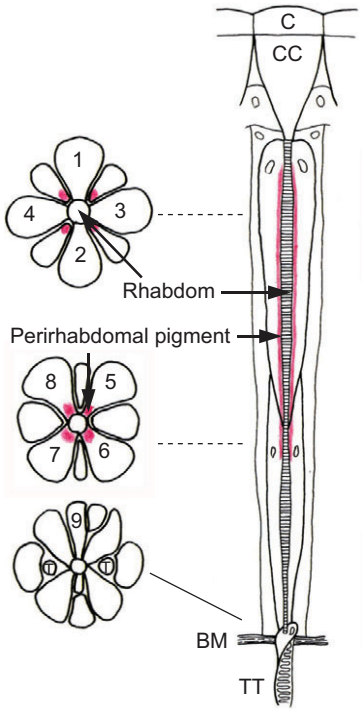

Fig. 1. Schematic diagram of a *Colias erate* ommatidium. Transverse views at three depths (left) at levels indicated in the longitudinal view (right). The numbers denote the nine photoreceptors, R1–9. The four distal photoreceptors, R1–4, contribute microvilli to the distal two-thirds of the rhabdom, while the proximal one-third is composed of four proximal photoreceptors, R5–8. The basal photoreceptor, R9, adds some microvilli at the basal end of the rhabdom. The rhabdom is surrounded by four clusters of perirhabdomal pigment, which are located in the cell bodies of the R5–8 photoreceptors; the cell bodies extend distally between the cell bodies of R1–4. C, cornea; CC, crystalline cone; BM, basement membrane; T, trachea; TT, tracheal tapetum.

discovered that the long-wavelength receptors peaking in the wavelength range longer than 600 nm, which are generically called 'red' receptors, are much more variable in females than in males, implying that females have an improved wavelength discrimination ability in the long wavelength region of the spectrum.

MATERIALS AND METHODS

Animals

Adults of the eastern pale clouded yellow butterfly, *Colias erate* (Esper 1805), were obtained from a laboratory culture derived from eggs laid by females captured around the Sokendai-Hayama campus, Kanagawa, Japan. Hatched larvae were reared under natural light conditions on fresh clover leaves.

Electrophysiology and dye injection

Electrophysiological methods were as described previously (Ogawa et al., 2012). Briefly, photoreceptor spectral sensitivities were determined by intracellular recording of responses to monochromatic stimuli delivered by a 500 W Xenon arc lamp *via* a series of narrow-band interference filters ranging from 300 to 740 nm. The light beam was focused on the tip of an optical fiber, the other end of which was attached to a Cardan-arm perimeter device in a Faraday cage, where it provided a point light source (1 deg in diameter). The quantum flux of each monochromatic stimulus was measured using a radiometer (Model-470D, Sanso, Tokyo, Japan) and adjusted to a standard number of photons using an optical wedge. For each experiment, a butterfly was mounted on a plastic stage in the Faraday cage, with its dorsal side up. A silver wire inserted into the head served as the reference electrode. A glass microelectrode filled with 10 mmol l^{-1} Alexa Fluor 568 (peak excitation/emission at 576/599 nm) in 200 mmol l^{-1} KCl (A10441, Molecular Probes, Invitrogen, Carlsbad, CA, USA), with a resistance of approximately 100 MΩ, was inserted into the retina through a small hole made in the cornea. Membrane potentials were recorded through a preamplifier (MEZ-7200; Nihon Kohden, Tokyo, Japan) connected to a computer *via* an AD converter (MP-150, BIOPAC Systems, Goleta, CA, USA).

After penetrating a photoreceptor, the optical fiber was adjusted so as to yield maximal responses. First, the spectral type of the impaled photoreceptor was determined using a series of monochromatic flashes of duration 30 ms, spaced 1 s apart. The response–stimulus intensity (V–log I) function was recorded over a 4 log unit intensity range at the photoreceptor's peak wavelength. The photoreceptor was subjected to further analyses only if the maximal response amplitude exceeded 30 mV. At the end of the recording, Alexa Fluor 568 was injected into the photoreceptor by applying a 2 nA hyperpolarizing DC current for ~5 min.

Anatomy

Immediately after the electrophysiological experiment, we observed the eyes with a fluorescence microscope (Olympus, BX50, Tokyo, Japan) applying 550 nm excitation light, and thus localized and photographed the ommatidium containing the dye-filled photoreceptor. We fixed the eyes in 4% paraformaldehyde in 0.1 mol sodium cacodylate buffer (pH 7.4) at room temperature for 30 min, then embedded the eyes in Quetol 812 (Nisshin EM, Tokyo, Japan) and made a series of 10-μm-thick transverse sections. Subsequently we identified the type of the ommatidium containing the dye-filled photoreceptor based on the pigmentation pattern (as revealed by normal transmitted light microscopy) combined with the fluorescence and eyeshine pattern of the intact eye. To determine the distribution of the perirhabdomal pigment along the rhabdom, we fixed intact eyes as described above and cut 5-μm-thick serial sections from the distal to the proximal end of the rhabdom.

Microspectrophotometry

The absorbance spectra of the perirhabdomal pigments were measured from pigment clusters in transverse light-microscopic sections using a microspectrophotometer consisting of a Leitz Ortholux microscope with an Olympus 20× objective (NA 0.46), connected to an Avaspec 2048-2 CCD detector array spectrometer (Avantes, Eerbeek, The Netherlands).

Model calculation

To quantitatively estimate the spectral sensitivity of the proximal photoreceptors of *C. erate*, we constructed an optical simulation model based on the anatomical details of the three types of ommatidia (I, II and III) present in the eye of *C. erate* (Arikawa et al., 2009). Based on the anatomical study of Arikawa et al. (Arikawa et al., 2009), we used the following values in the model calculations. The total length of the rhabdom was 500 μm (Fig. 2). The depth of the upper tier of the rhabdom, with rhabdomeres of photoreceptors R1–4, was 250 μm in type I ommatidia, and 200 μm in type II and III ommatidia. The depth of the second tier (containing the rhabdomeres of photoreceptors R5–8) was the remaining part of the rhabdom, except for the basal 10 μm, which was assumed to be fully

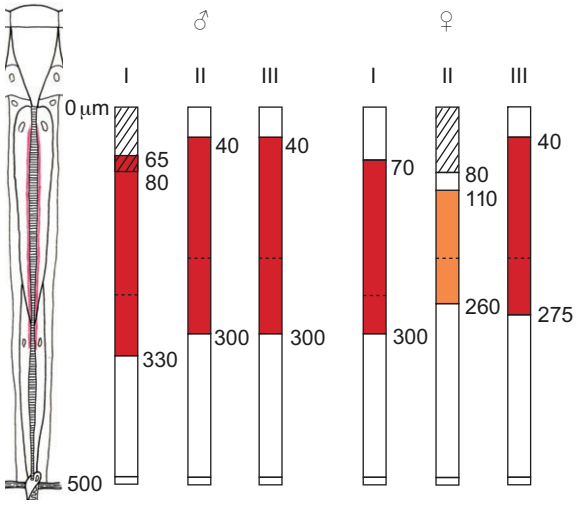

Fig. 2. Diagram of the dimensions assumed in the optical modeling of the rhabdom. Left: diagram of an ommatidium of *Colias erate*. Right: simple compartment models of the rhabdoms in ommatidial types I–III of male and female *C. erate*. The total length of each rhabdom was assumed to be 500 μm, with the distal tier occupying 250 μm in type I ommatidia and 200 μm in type II and III ommatidia. The distribution pattern of the perirhabdomal pigments (red in all ommatidia except in the ommatidial type II of the female, see Fig. 3) depends on the type of ommatidium and the sex, as indicated. Diagonal lines show the location of fluorescent pigment in the male type I and the female type II ommatidia.

occupied by the rhabdomere of R9. A fluorescent pigment, whose absorbance spectrum was assumed to be identical to that of the fluorescent pigment in *P. rapae* (Arikawa et al., 2005), was present in the most distal 80 μm of the rhabdoms in type I ommatidia in male eyes and type II ommatidia of female eyes (Ogawa et al., 2012). The visual pigment expressed in each photoreceptor (Awata et al., 2009; Ogawa et al., 2012) and the occupancy ratio of the rhabdomeres in the entire rhabdom (Arikawa et al., 2009) are shown in Table 1. Visual pigment absorbance spectra were calculated using the Govardovskii template (Govardovskii et al., 2000). We applied the simple model approach of Stavenga and Arikawa (Stavenga and Arikawa, 2011) and thus ignored the wave-optical properties of the dioptric system and rhabdom. The transmittance of a rhabdom layer with thickness Δz is given by:

$$T(\lambda) = \exp[-\kappa(\lambda)\Delta z], \quad (1)$$

with:

$$\kappa(\lambda) = \kappa_V(\lambda) + \kappa_S(\lambda), \quad (2)$$

where κ_V is the local absorbance coefficient due to absorption by the visual pigments, which is given by:

$$\kappa_V = \kappa_{V,max}[\Sigma\alpha_i(\lambda)\rho_i], \quad (3)$$

where $\kappa_{V,max}$ is the peak absorbance coefficient, α_i is the normalized absorbance spectrum of the visual pigment in photoreceptor Ri (i=1–8) and ρ_i is the occupancy ratio of the rhabdomere of photoreceptor Ri in the rhabdom. κ_S from Eqn 2 represents the absorbance coefficient of the fluorescent pigment as well as the perirhabdomal pigment:

$$\kappa_S = \kappa_{S,max}\alpha_S(\lambda), \quad (4)$$

where $\kappa_{S,max}$ is the peak absorbance coefficient and α_S is the normalized absorbance spectrum. The light flux at location z, $I(z,\lambda)$, is reduced into that at location $z + \Delta z$, $I(z+\Delta z)$, by:

$$I(z+\Delta z,\lambda) = T(\lambda)I(z,\lambda). \quad (5)$$

The light flux absorbed by the visual pigment of the individual photoreceptors in a compartment of depth Δz is given by:

$$\Delta A_i(\lambda) = [I(z,\lambda) - I(z+\Delta z,\lambda)]\ \kappa_{V,max}\alpha_i(\lambda)\rho_i / \kappa(\lambda). \quad (6)$$

We assumed that at all wavelengths a unit light flux entered the ommatidia. Before reaching the photoreceptors, the incident light first passes the dioptric apparatus, consisting of the corneal facet lens and crystalline cone. We assumed that the transmittance of the dioptric apparatus was equivalent to that of the moth *Endromis* (Bernhard et al., 1965). Its transmittance spectrum, $T_C(\lambda)$, is thus identical to $I(0,\lambda)$, the relative light flux spectrum at z=0 μm, the tip of the rhabdom. Summing the absorbed light fractions of the individual photoreceptors over the different rhabdom compartments then yields the photoreceptor's absorbance spectrum. Normalizing this yields the spectral sensitivity.

RESULTS

Sexually dimorphic perirhabdomal pigment

The ommatidia of *C. erate* can be divided into three types, I–III, according to their characteristic patterns of perirhabdomal pigmentation (Fig. 3). In a previous study on male *C. erate* (Arikawa et al., 2009), we reported that the perirhabdomal pigments of all three ommatidial types have the same red color (Fig. 3A). However, further anatomical studies revealed that in the female the pigment in type II ommatidia is orange (Fig. 3B).

We measured the absorbance spectra of the perirhabdomal pigments by microspectrophotometry. The absorbance spectra of the red pigment clusters of males and females were virtually identical, but the spectrum of the orange pigment in female type II ommatidia was different (Fig. 3C). Because our microspectrophotometer did not allow reliable measurements in the ultraviolet range, the spectra were assumed to be constant below 366 nm; in fact, the absorbance of the pigments in the UV wavelength region had a negligible effect on the sensitivity of the red receptors. The mean spectra of Fig. 3C were used in the model calculations.

The perirhabdomal pigments are located near the rhabdom in the soma of the proximal photoreceptors, R5–8. To investigate the distribution of the pigments along the rhabdom, we examined a series

Table 1. Parameters used in the model

	$\kappa_{S,max}$		Visual pigment absorption peak (nm)/rhabdomere occupancy ratio			
	♂	♀	R1	R2	R3, 4	R5–8
Type I	3.0	2.5	360/0.40	430/0.40	565/0.15	565/0.25
Type II	2.8	1.0	430+460/0.35	430+460/0.35	565/0.15	565/0.25
Type III	3.0	4.0	360/0.35	360/0.35	565/0.15	565/0.25

$\kappa_{S,max}$, peak absorbance coefficient of red pigment.

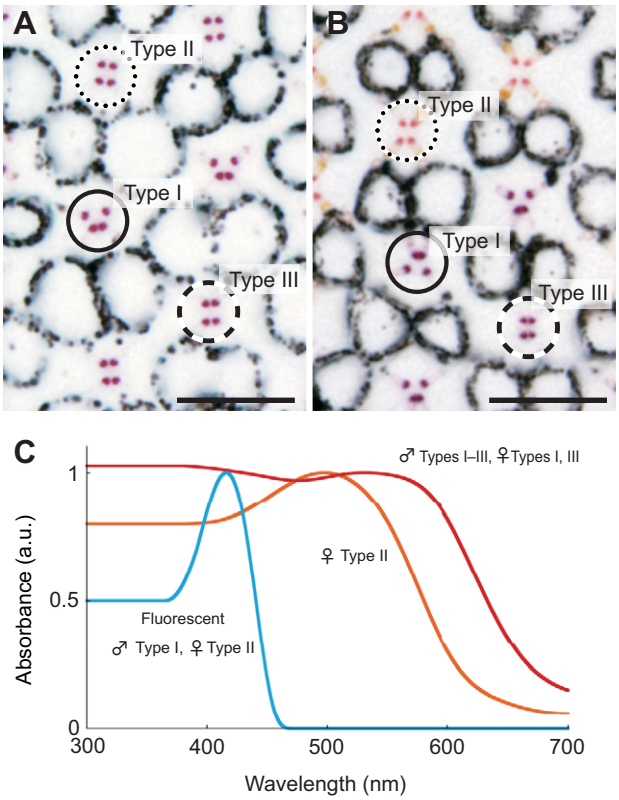

Fig. 3. Sexual dimorphism of the perirhabdomal pigments. (A) Light microscopic unstained plastic transverse section through the distal tier of the ventral part of the eye of a male *Colias erate*, showing pigment clusters arranged in trapezoidal (solid circle, type I ommatidium), square (dotted circle, type II) and hexagonal patterns (dashed circle, type III). In all three ommatidial types the pigment is red. (B) A similar section of the female ventral eye, showing the same three patterns of pigment clusters. However, the pigment in ommatidial type II is orange. (C) Averaged, normalized absorbance spectra of the red and orange perirhabdomal pigments, measured with a microspectrophotometer. The spectrum of the fluorescing pigment is from Stavenga and Arikawa (Stavenga and Arikawa, 2011). Scale bars, 20 μm.

of 5-μm-thick plastic sections of eyes of both sexes. The pigmented regions differed between the ommatidial types (Fig. 2). The orange-pigmented region of the female type II ommatidia is shorter (150 μm) than the region of the red pigment in the other ommatidial types (230 μm), indicating weaker filtering by the orange pigment. In both sexes, the pigment in type I ommatidia extends slightly deeper than in type II and III ommatidia (Fig. 2).

Spectral sensitivities of proximal photoreceptors

We measured the spectral sensitivities of the proximal photoreceptors, R5–8, in all three types of ommatidia in the ventral region of both male and female eyes. Of the more than 100 recordings, 28 photoreceptors were successfully labeled and thus analyzed in detail. Fig. 4 shows examples of labeled photoreceptors from each ommatidial type of each sex. For each of the photoreceptors, the top, middle and bottom panels, respectively, show the spectral sensitivity, the ommatidial array as observed with regular transmission light microscopy, and the array as observed with fluorescence microscopy revealing the Alexa-Fluor-filled photoreceptor cell body.

All photoreceptors in Fig. 4 are maximally sensitive in the wavelength region above 600 nm and are therefore collectively called 'red' receptors. However, the spectral sensitivity profiles in the different ommatidial types differ from each other in both sexes. For example, in type I ommatidia, the male R5 photoreceptor (Fig. 4A) has its main peak at 680 nm and a large secondary peak at 480 nm, while the female R5 (Fig. 4D) exhibits a single peak at 640 nm. Similarly, a large secondary sensitivity peak exists in type II ommatidia only in males (Fig. 4B,E). In Fig. 5, we distinguish these red (R) receptors by adding the sex, male (m) or female (f), and the ommatidial type, I, II or III; e.g. RmI indicates a red receptor in type I ommatidia of males and RfII is a red receptor in type II ommatidia of females.

Model calculations

Fig. 5 shows averaged spectral sensitivities of the various classes of red receptors, which were localized by dye injection and identified by anatomy. We use the averaged spectral sensitivities as the representatives of the red receptors of the different ommatidial types.

In our previous paper on the distal R1–4 photoreceptors of *C. erate*, we could quantitatively describe the measured spectral sensitivities with a simple (heuristic) model of the distal rhabdom tier (Ogawa et al., 2012). We extended this model by including the proximal tier in order to quantitatively estimate the spectral sensitivity of R5–8 photoreceptors. Fig. 5 shows the means of the spectral sensitivities (symbols) measured in the photoreceptors of the different ommatidial types of male and female together with calculated spectra (continuous curves) obtained by using the following parameter values. All visual pigments had a peak absorbance coefficient $\kappa_{V,max}=0.005\,\mu m^{-1}$. The peak absorbance coefficient of the fluorescent pigment in male type I and female type II ommatidia was $\kappa_{S,max}=0.02\,\mu m^{-1}$. The peak absorbance coefficients of the perirhabdomal pigment, with absorbance spectra given by Fig. 3C, are shown in Table 1; the longitudinal density distribution as shown in Fig. 2 was assumed to be constant. The visual pigment CeL (Awata et al., 2009), expressed in all proximal photoreceptors, was R565, i.e. its peak absorption was at 565 nm (Ogawa et al., 2012). Modifying the assumed parameter values in a realistic range did not essentially change the results.

The model successfully reproduced the profile of the main sensitivity band of all proximal photoreceptors. In males, the peak wavelength of the calculated spectra is 660 nm in all ommatidial types (Fig. 5A–C). In females, it is 650 nm in type I (Fig. 5D), 610 nm in type II (Fig. 5E) and 660 nm in type III (Fig. 5F). Although male and female type I ommatidia have the same red pigment and rhabdoms of similar dimensions, the spectral sensitivities of the proximal photoreceptors differ due to a difference in length of the pigmented region, which is approximately 35 μm shorter in females (Fig. 2).

The present model did not reproduce the secondary sensitivity bands in the short wavelength region, showing that the model is incomplete, as will be discussed below.

DISCUSSION

Red receptors in *Colias erate*

We characterized the spectral sensitivities of the proximal photoreceptors in the compound eye of *C. erate* by intracellular recording and optical modeling. All photoreceptors were maximally sensitive in the red wavelength region, but their peak wavelengths differed strikingly between males and females. According to the actual recordings and model calculations, we conclude that the proximal photoreceptors of males peak at 660 nm in all ommatidial types, and those in females peak at 610, 650 or 660 nm depending on the ommatidial type. To the best of our knowledge, 660 nm is the longest peak wavelength of any red receptor reported in an insect.

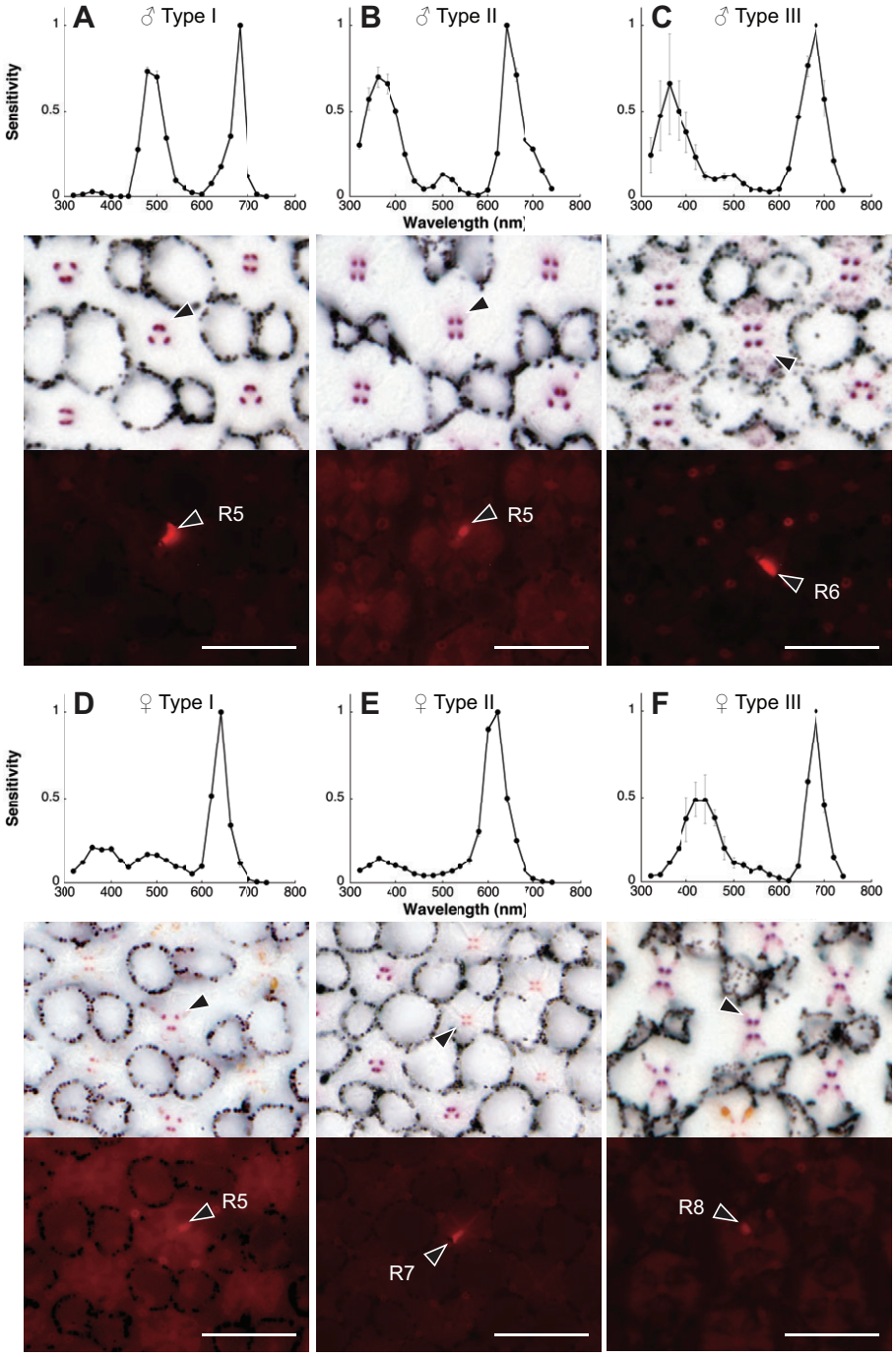

Fig. 4. Six examples of proximal photoreceptors of *Colias erate*. The top rows show spectral sensitivity, the middle rows show transmission light micrographs of the photoreceptor (arrowheads) in the ommatidial array and the bottom rows show its fluorescence image (arrowheads). (A) Male R5 in a type I ommatidium. (B) Male R5 in a type II ommatidium. (C) Male R6 in a type III ommatidium. (D) Female R5 in a type I ommatidium. (E) Female R7 in a type II ommatidium. (F) Female R8 in a type III ommatidium. Scale bars, 20 μm.

This is also the first example of a distinct sexual dimorphism of red receptors in any animal.

The simple model we applied could well reproduce the principal sensitivity peaks of the red receptors. Two mechanisms appeared to account for the differences in the calculated sensitivity spectra. First, the different absorbance spectra of the red and orange pigment clusters mean that different spectral filters act on the proximal photoreceptors (Figs 2, 3). Second, the orange pigment in the female type II ommatidia extends over just 150 μm (Fig. 2), which is much shorter than in the other ommatidia, resulting in a lower density of the pigment filter. Accordingly, the proximal photoreceptors in female type II ommatidia have the shortest peak wavelength (620 nm). Furthermore, the extent of red pigment in type I ommatidia is longer in males (265 μm) than in females (230 μm). Consequently, the spectral sensitivity of the proximal photoreceptors in type I ommatidia peaks at 660 nm in the male and at 640 nm in the female.

The modeled spectra deviate markedly from the experimental spectra in the short- and middle-wavelength range, where the calculations predict a low sensitivity but the measured spectra show distinct sensitivity bands (Fig. 5). The same problem was encountered in our study of the small white butterfly, *P. rapae*. In that instance, calculations with a similar simple model also yielded low sensitivities in the short and middle wavelength range. An elaborate wave-optical model of the *P. rapae* rhabdom produced substantial sensitivity bands in the shorter wavelength

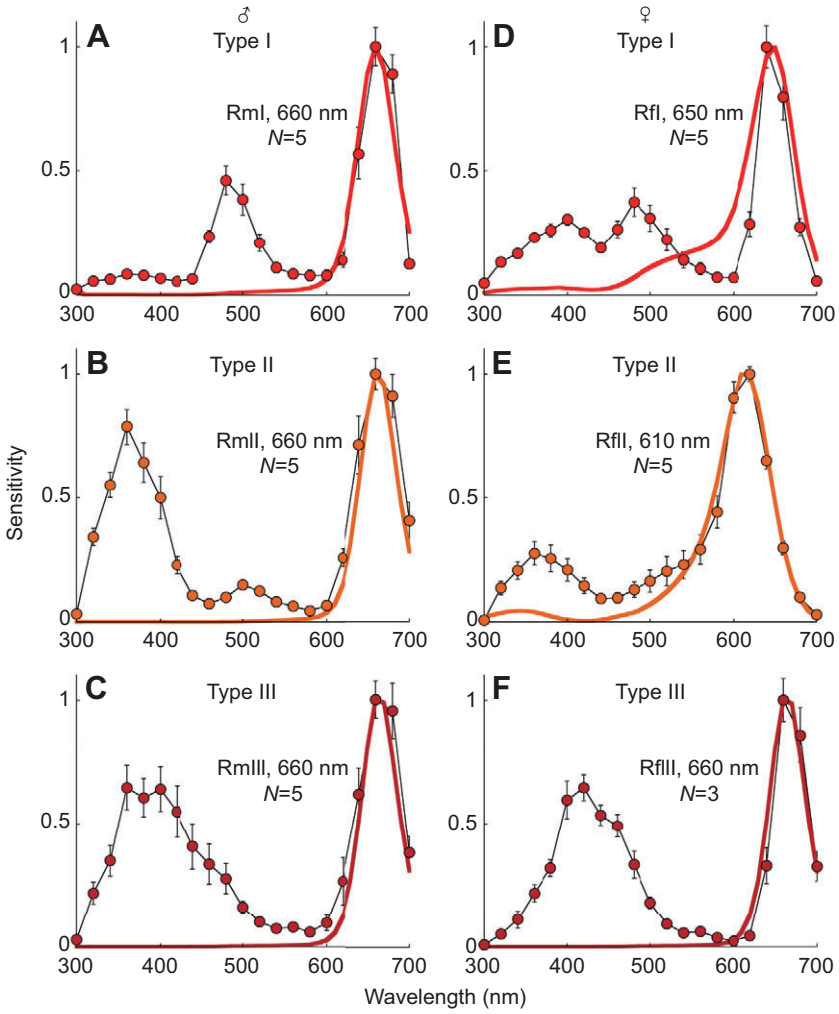

Fig. 5. Spectral sensitivities of proximal photoreceptors (mean ± s.e.m.; *N*, number of samples) with model calculations (colored curves). Each panel indicates the photoreceptor nomenclature, peak wavelength of the calculated spectrum and number of samples. (A) Mean spectral sensitivities of red receptors in male type I ommatidia, RmI. (B) Male type II, RmII. (C) Male type III, RmIII. (D) Female type I, RfI. (E) Female type II, RfII. (F) Female type III, RfIII.

range (Stavenga and Arikawa, 2011). Our attempts to construct a wave-optical model similar to that of *P. rapae* have remained somewhat unsatisfactory, due to the considerably more complicated structure of the rhabdoms of *C. erate*; whereas the rhabdoms of *P. rapae* approximate a homogeneously tapering cylinder, the rhabdoms of *C. erate* have a pronounced constriction in the middle (Arikawa et al., 2009). At the constriction, the rhabdomeric microvilli are locally replaced by concentrated red pigment. This makes wave-optical modeling difficult, because the rhabdoms' waveguide properties strongly depend on both the rhabdom diameter and the refractive indices of the medium within and surrounding the rhabdom, which is unknown in the case of the red pigment. Nevertheless, preliminary modeling attempts yielded clear sensitivity bands in the short and middle wavelength range. From this observation, together with the exemplary case of *P. rapae*, it seems reasonable to hypothesize that the ultraviolet and blue sensitivity bands of the proximal photoreceptors of *C. erate* (Fig. 5) are due to waveguide effects.

Note that the RmI and RfI are similar in the principal peaks in red wavelength region, but the secondary sensitivity band in the UV–V wavelength region is smaller in RmI than in RfI (Fig. 5A,D). In type II red receptors, the relationship is reverse. This sexual difference is attributable, at least in part, to the sexually dimorphic distribution of the fluorescence pigment (Fig. 3C): the male type I and the female type II ommatidia contain the fluorescence pigment (Ogawa et al., 2012).

Function of the multiple red receptors

Remarkably, the expression pattern of visual pigments is identical in both sexes of *C. erate* (Awata et al., 2009; Ogawa et al., 2012), but the spectral sensitivities of their photoreceptor sets differ. Sexual dimorphism in photoreceptor spectral sensitivities was already encountered in the distal photoreceptors of *Colias* (Ogawa et al., 2012). A fluorescent pigment that absorbs maximally at around 420 nm, concentrated near the distal tip of the rhabdom in male type I ommatidia and female type II ommatidia, produces shouldered-blue receptors (sB) in males and narrow-blue receptors (nB) in females (Fig. 6) (see Ogawa et al., 2012). Together with the present study, this shows that the sexual dimorphism of *C. erate* eyes is rather pronounced (Fig. 6, Table 2). It is therefore most likely that males and females view the colored world quite differently. The eyes' set of spectral photoreceptors provides an animal with the ability to see color and/or to discriminate light sources that differ in wavelength. Extensive studies of wavelength discrimination in the honeybee *Apis mellifera* (von Helversen, 1972) demonstrated that the threshold for wavelength discrimination (that is, the minimal discriminable wavelength difference) is the lowest at wavelengths in between the sensitivity peaks of the trichromatic set of photoreceptors (Kelber et al., 2003). The eye of the Japanese yellow swallowtail butterfly, *Papilio xuthus*, has eight classes of photoreceptor, distributed in three types of ommatidia. Behavioral tests revealed that the wavelength discrimination acuity of *P. xuthus* is maximal at 420, 480 and 560 nm. Assuming a spectral opponency

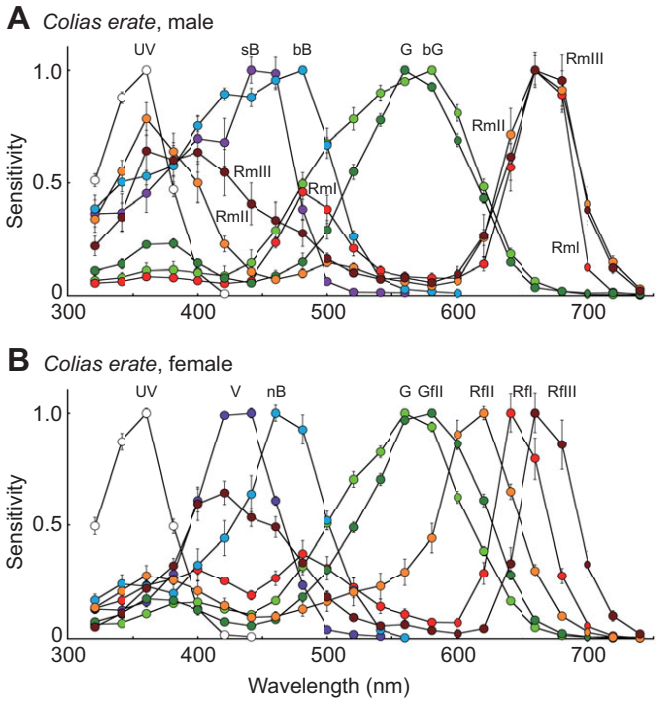

Fig. 6. Spectral sensitivities of all photoreceptor classes in males (A) and females (B) of *Colias erate*. The photoreceptors are divided into ultraviolet (UV), blue (V, nB, sB, bB), green [G, bG, GfII (green in female type II)] and red (RmI, RmII, RmIII, RfI, RfII, RfIII) classes. The blue and red receptor classes are sexually dimorphic.

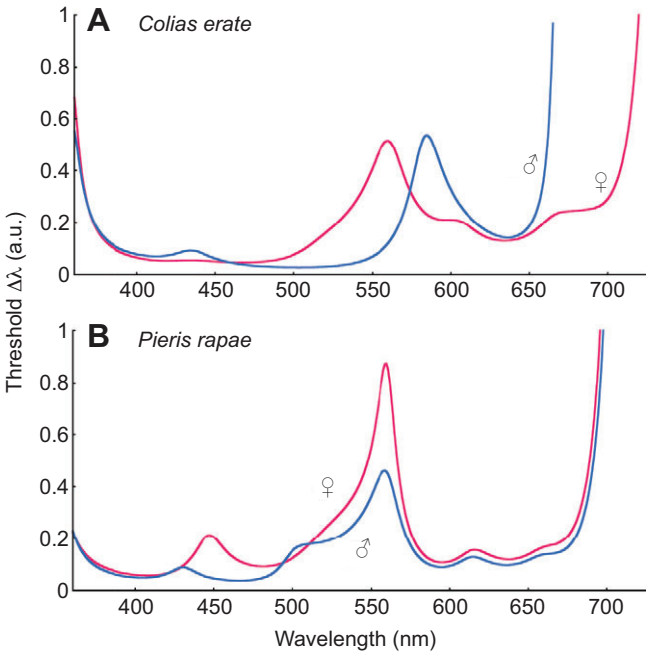

Fig. 7. Wavelength discrimination threshold (arbitrary units) predicted by a receptor noise-limited color opponent model. (A) Threshold for male and female *Colias erate* when all photoreceptors are assumed to participate. (B) Threshold for male and female *Pieris rapae*.

mechanism between the spectral receptors through the interphotoreceptor connections in the lamina (Takemura and Arikawa, 2006), we applied the receptor noise-limited color opponent model (Vorobyev and Osorio, 1998) to identify the photoreceptors that were involved in the wavelength discrimination behavior in *P. zuthus*. We thus found that only four spectral classes of photoreceptors participate in wavelength discrimination, i.e. *P. zuthus* is tetrachromatic (Koshitaka et al., 2008).

The sexual dimorphism of the spectral photoreceptors of *C. erate* implies that wavelength discrimination differs between the two sexes. To investigate this wavelength discrimination ability, we have applied the receptor noise-limited color opponent model (Vorobyev and Osorio, 1998) to the *C. erate* visual system (Fig. 7A). For comparison, we performed the same analysis for the visual system of *P. rapae* (Fig. 7B). We assumed that all spectral receptors of an eye participate in the wavelength discrimination system. Because in *C. erate* males the sensitivities of all red receptors peak at 660 nm, wavelengths above approximately 650 nm cannot be distinguished (Fig. 7A, blue line). In contrast, *C. erate* females have a set of three red receptors, which extends their discriminable range to much longer wavelengths up to approximately 700 nm (Fig. 7A, red line). Both male and female *P. rapae* have the same two types of red receptor, R (620 nm) and dR (640 nm) (Qiu and Arikawa, 2003). In both sexes wavelength discrimination in the red wavelength range is similar, extending to about 670 nm (Fig. 7B). Clearly, *C. erate* females should have the best spectral resolution in the longer wavelength range.

Table 2. Characteristics of the three types of ommatidia of the *Colias erate* ventral eye

				Photoreceptor spectral sensitivity/opsin mRNA			
		Pigment	Fluorescence	R1	R2	R3, 4	R5–8
Type I	♂	Red	+	UV	sB	bG	RmI
	♀	Red	–	UV	V	G	RfI
				CeUV	*CeV1+V2*	*CeL*	
Type II	♂	Red	–	bB		G	RmII
	♀	Orange	+	nB		GfII	RfII
				CeV1+V2+B		*CeL*	
Type III	♂	Red	–	UV		G	RmIII
	♀	Red	–	UV		G	RfIII
				CeUV		*CeL*	

Photoreceptor nomenclature: UV, ultraviolet; V, violet; sB, shouldered-blue; bB, broad-blue; G, green; bG, broad-green; GfII, green in female type II ommatidia; Rm(f)I(II,III), red of male (female) type I (II, III) ommatidia. See Fig. 6 for the spectral sensitivity curves. For opsins, see Awata et al. (Awata et al., 2009) and Ogawa et al. (Ogawa et al., 2012).

Red receptors are presumably crucial for female lycaenids to identify larval food sources (Bernard and Remington, 1991). Similarly, the ovipositing Australian orchard butterfly, *Papilio aegeus*, uses a red receptor peaking at 610 nm to select young green leaves as being the best food for larvae (Kelber, 1999a). These examples suggest the hypothesis that the three red receptors of *Colias* females are highly beneficial for detecting suitable leaves for oviposition. The light reflected by leaves is highest in the green and red ranges, but weaker additional reflections occur at shorter wavelengths. The sensitivity bands of the photoreceptors in the short- and middle-wavelength ranges (Fig. 5) will hence create a non-negligible background signal, but the high red sensitivity – especially the strongly red-shifted spectral sensitivity of the proximal photoreceptors in female type III ommatidia – will enable the discrimination of subtle differences in leaf coloration. Some of the spectral receptors of *C. erate* have high polarization sensitivity as well (Pirih et al., 2010), which might enhance the spectral discrimination as in the case of *Papilio* (Kelber, 1999b). Of course, not all spectral receptors necessarily contribute to the wavelength discrimination process, as is exemplified by *P. xuthus* (Koshitaka et al., 2008). Elucidation of the actual wavelength discrimination ability of *Colias* will require behavioral experiments.

Regionalization and sexual dimorphism of the *Colias erate* retina

The eye of *C. erate* has a clear discontinuity between the dorsal third and the ventral two-thirds (Awata et al., 2009). The dorsal region is characterized by its light pigmentation (Arikawa et al., 2009) and the absence of the blue-absorbing visual pigment CeB (Ogawa et al., 2012). We have performed some preliminary studies to investigate whether the dorsal photoreceptors are also sexually dimorphic. However, intracellular recordings did not reveal any sexual dimorphism in the distal nor proximal tiers of the dorsal retina. The proximal photoreceptors in the dorsal region of both sexes were maximally sensitive at 600–620 nm, and the spectral sensitivity curves had no secondary peak sensitivities in the shorter wavelength range (cf. Fig. 5E). This is presumably due to the low density of perirhabdomal pigments, resulting in only moderate filtering. The experimental results indicated that the dorsal eyes of both males and females have the same, rather simple set of UV, V, G and R receptors. Possibly, the visual system of the dorsal retina mediates general visual activities, such as flight control and evading predators. The ventral retina may have evolved to mediate sexual behaviors including courtship and oviposition.

ACKNOWLEDGEMENTS

We thank Drs Hisashi Otsuki and Hisaharu Koshitaka for extensive discussion, and Dr Finlay Stewart for editing the English.

AUTHOR CONTRIBUTIONS

Y.O. designed the study, performed all the experiments and wrote the paper. M.K. contributed to the design of the study and performed electrophysiological and histological experiments in part. D.G.S. measured the spectra shown in Fig. 3C, and contributed to the modeling of photoreceptor spectral sensitivities and the writing of the paper. K.A. contributed to the design of the study, performed histology in part and contributed to the writing of the paper. This work is a part of the PhD thesis of Y.O.

COMPETING INTERESTS

No competing interests declared.

FUNDING

Y.O. was a recipient of a Japan Society for the Promotion of Science (JSPS) graduate student fellowship, DC2. This study was supported in part by a JSPS Grant-in-Aid for Scientific Research [no. 21247009 to K.A.], a grant from the Ministry of Agriculture, Forestry and Fisheries of Japan (MAFF) [Elucidation of biological mechanisms of photoresponse and development of advanced technologies utilizing light; grant no. INSECT-1101 to K.A.], and a grant from the Air Force Office of Scientific Research/European Office of Aerospace Research and Development (AFOSR/EOARD) [grant FA8655-12-1-2053 to D.G.S.].

REFERENCES

Arikawa, K. and Stavenga, D. G. (1997). Random array of colour filters in the eyes of butterflies. *J. Exp. Biol.* **200**, 2501-2506.

Arikawa, K., Wakakuwa, M., Qiu, X., Kurasawa, M. and Stavenga, D. G. (2005). Sexual dimorphism of short-wavelength photoreceptors in the small white butterfly, *Pieris rapae crucivora*. *J. Neurosci.* **25**, 5935-5942.

Arikawa, K., Pirih, P. and Stavenga, D. G. (2009). Rhabdom constriction enhances filtering by the red screening pigment in the eye of the eastern pale clouded yellow butterfly, *Colias erate* (Pieridae). *J. Exp. Biol.* **212**, 2057-2064.

Awata, H., Wakakuwa, M. and Arikawa, K. (2009). Evolution of color vision in pierid butterflies: blue opsin duplication, ommatidial heterogeneity and eye regionalization in *Colias erate*. *J. Comp. Physiol. A* **195**, 401-408.

Bernard, G. D. and Miller, W. H. (1970). What does antenna engineering have to do with insect eyes? *IEEE Student J.* **8**, 2-8.

Bernard, G. D. and Remington, C. L. (1991). Color vision in *Lycaena* butterflies: spectral tuning of receptor arrays in relation to behavioral ecology. *Proc. Natl. Acad. Sci. USA* **88**, 2783-2787.

Bernhard, C. G., Miller, W. H. and Møller, A. R. (1965). The insect corneal nipple array. *Acta Physiol. Scand.* **63 Suppl. 243**, 1-79.

Govardovskii, V. I., Fyhrquist, N., Reuter, T., Kuzmin, D. G. and Donner, K. (2000). In search of the visual pigment template. *Vis. Neurosci.* **17**, 509-528.

Kelber, A. (1999a). Ovipositing butterflies use a red receptor to see green. *J. Exp. Biol.* **202**, 2619-2630.

Kelber, A. (1999b). Why 'false' colours are seen by butterflies. *Nature* **402**, 251.

Kelber, A., Vorobyev, M. and Osorio, D. (2003). Animal colour vision – behavioural tests and physiological concepts. *Biol. Rev. Camb. Philos. Soc.* **78**, 81-118.

Koshitaka, H., Kinoshita, M., Vorobyev, M. and Arikawa, K. (2008). Tetrachromacy in a butterfly that has eight varieties of spectral receptors. *Proc. Biol. Sci.* **275**, 947-954.

Ogawa, Y., Awata, H., Wakakuwa, M., Kinoshita, M., Stavenga, D. G. and Arikawa, K. (2012). Coexpression of three middle wavelength-absorbing visual pigments in sexually dimorphic photoreceptors of the butterfly *Colias erate*. *J. Comp. Physiol. A* **198**, 857-867.

Pirih, P., Arikawa, K. and Stavenga, D. G. (2010). An expanded set of photoreceptors in the eastern pale clouded yellow butterfly, *Colias erate*. *J. Comp. Physiol. A* **196**, 501-517.

Qiu, X. and Arikawa, K. (2003). Polymorphism of red receptors: sensitivity spectra of proximal photoreceptors in the small white butterfly *Pieris rapae crucivora*. *J. Exp. Biol.* **206**, 2787-2793.

Stavenga, D. G. and Arikawa, K. (2011). Photoreceptor spectral sensitivities of the small white butterfly *Pieris rapae crucivora* interpreted with optical modeling. *J. Comp. Physiol. A* **197**, 373-385.

Takemura, S. Y. and Arikawa, K. (2006). Ommatidial type-specific interphotoreceptor connections in the lamina of the swallowtail butterfly, *Papilio xuthus*. *J. Comp. Neurol.* **494**, 663-672.

Takemura, S. Y., Stavenga, D. G. and Arikawa, K. (2007). Absence of eye shine and tapetum in the heterogeneous eye of *Anthocharis* butterflies (Pieridae). *J. Exp. Biol.* **210**, 3075-3081.

von Helversen, O. (1972). Zur spektralen unterschiedsempfindlichkeit der honigbiene. *J. Comp. Physiol. A* **80**, 439-472.

Vorobyev, M. and Osorio, D. (1998). Receptor noise as a determinant of colour thresholds. *Proc. Biol. Sci.* **265**, 351-358.

Wakakuwa, M., Stavenga, D. G., Kurasawa, M. and Arikawa, K. (2004). A unique visual pigment expressed in green, red and deep-red receptors in the eye of the small white butterfly, *Pieris rapae crucivora*. *J. Exp. Biol.* **207**, 2803-2810.